



Integrated Ferroelectrics

An International Journal

ISSN: (Print) (Online) Journal homepage: <https://www.tandfonline.com/loi/ginf20>

Investigations on Electrical Properties of Al₂O₃, ZnO and MgO Doped Ba_{0.7}Sr_{0.3}TiO₃ Ceramics Based MIM Capacitor for Energy Storage Application

P. S. Smitha, V. Suresh Babu & G. Shiny

To cite this article: P. S. Smitha, V. Suresh Babu & G. Shiny (2021) Investigations on Electrical Properties of Al₂O₃, ZnO and MgO Doped Ba_{0.7}Sr_{0.3}TiO₃ Ceramics Based MIM Capacitor for Energy Storage Application, Integrated Ferroelectrics, 213:1, 194-208, DOI: [10.1080/10584587.2020.1860604](https://doi.org/10.1080/10584587.2020.1860604)

To link to this article: <https://doi.org/10.1080/10584587.2020.1860604>



Published online: 28 Feb 2021.



Submit your article to this journal [↗](#)



Article views: 19






View related articles [↗](#)



View Crossmark data [↗](#)



Investigations on Electrical Properties of Al₂O₃, ZnO and MgO Doped Ba_{0.7}Sr_{0.3}TiO₃ Ceramics Based MIM Capacitor for Energy Storage Application

P. S. Smitha^a , V. Suresh Babu^b , and G. Shiny^c 

^aDepartment of Electronics and Communication Engineering, College of Engineering Trivandrum, APJ Abdul Kalam Technological University, Kerala, India; ^bDepartment of Electronics and Communication Engineering, Government Engineering College Wayanad, APJ Abdul Kalam Technological University, Kerala, India; ^cDepartment of Electronics and Communication Engineering, Government College of Engineering Kannur, APJ Abdul Kalam Technological University, Kerala, India

ABSTRACT

In this paper, the performance parameters, capacitance and leakage current of Al₂O₃, ZnO and MgO doped Ba_{0.7}Sr_{0.3}TiO₃ ceramics based metal-insulator-metal (MIM) capacitors are investigated. The specific capacitance of intrinsic Ba_{0.7}Sr_{0.3}TiO₃ ceramic based MIM capacitor changes with frequency whereas Al₂O₃ doped Ba_{0.7}Sr_{0.3}TiO₃ ceramics based MIM capacitor exhibits almost frequency independent specific capacitance. 2.0 wt% ZnO doped Ba_{0.7}Sr_{0.3}TiO₃ ceramics based MIM capacitor exhibits highest specific capacitance. The doping of Ba_{0.7}Sr_{0.3}TiO₃ ceramics with ZnO is not sufficient for enhancing leakage current performance. On investigation, 4.0 wt% MgO doped Ba_{0.7}Sr_{0.3}TiO₃ ceramics based MIM capacitor is found better for energy storage application.

ARTICLE HISTORY

Received 7 August 2020
Accepted 2 December 2020

KEYWORDS

Energy storage; ceramic capacitor; doping; specific capacitance; leakage current

1. Introduction

The key features of an energy storage device are specific capacitance and leakage current. MIM capacitor is a better storage device as it possess 100% charge-discharge efficiency since no chemical reactions are involved. High-k material such as BST is a good candidate for insulator in Ba_{0.7}Sr_{0.3}TiO₃ ceramic based MIM capacitors and found to possess high specific capacitance and relatively high leakage current. Doping of Ba_{0.7}Sr_{0.3}TiO₃ ceramic with suitable insulator material is one of the effective solutions for enhancing leakage current performance of Ba_{0.7}Sr_{0.3}TiO₃ ceramic based MIM capacitors, thereby making it suitable for energy storage application. The dopant ions can replace ‘A’ or ‘B’ sites of ABO₃ in (Ba_{0.7}Sr_{0.3})(Ti)O₃ structure depending on ionic radii of dopants, keeping A:B ratio of one and the dielectric properties of ceramic capacitors are much affected when acceptor ions replace ‘B’ sites [1].

When BST is doped with materials having low relative permittivity such as MnO, MgO, Al₂O₃, Nb₂O₅ and La₂O₃, compositional inhomogeneities on a nano-scale results in reducing overall relative permittivity. Liang et al. [2] observed an enhancement in

CONTACT P. S. Smitha  smithaps@cet.ac.in  Department of Electronics and Communication Engineering, College of Engineering Trivandrum, APJ Abdul Kalam Technological University, Kerala, India

relative permittivity when BST is doped with 0.1 mol% Mn than intrinsic BST due to low compositional inhomogeneities at low doping concentration. As doping concentration of MnO increases, relative permittivity starts to decrease which indicates that a vital controlling factor of relative permittivity is compositional inhomogeneity.

One of the reasons for dielectric loss in BST ceramic is the jumping of electrons from one Ti ion to another in ABO_3 perovskite structure [3]. Being acceptor dopants, Al^{3+} , Zn^{2+} and Mg^{2+} ions can occupy the B sites of Ti^{4+} ion. The appropriate concentrations of these dopant ions absorb the electron jumps between Ti ions and hence prevent Ti^{4+} to Ti^{3+} reduction thereby reducing dielectric loss [4].

The dielectric properties of $Ba_{0.7}Sr_{0.3}TiO_3$ ceramics when doped with Al_2O_3 , ZnO and MgO are investigated. The dopant solubility in $BaSrTiO_3$ ceramics depends mainly on its ionic radius [5]. The ionic radii of Ba^{2+} , Sr^{2+} and Ti^{4+} are 1.36 \AA , 1.16 \AA [1] and 0.68 \AA [6] respectively. The ionic radii of Al^{3+} , Zn^{2+} and Mg^{2+} ions are 0.675 \AA , 0.88 \AA and 0.86 \AA respectively [7] which are comparable to that of Ti^{4+} . This enhances the chances for Al^{3+} , Zn^{2+} and Mg^{2+} ions to replace Ti^{4+} ions in BST during the process of doping.

The melting points of Al_2O_3 , ZnO and MgO are 2072°C , 1975°C and 2852°C which are well below the sintering temperature of BST samples (1275°C). The performance parameters such as specific capacitance as well as leakage current of MIM capacitor with Al_2O_3 , ZnO and MgO doped $Ba_{0.7}Sr_{0.3}TiO_3$ ceramics as insulator materials are measured. The leakage current behavior is studied with x-ray powder diffraction patterns as well.

2. Experimental Procedure

The $Ba_{0.7}Sr_{0.3}TiO_3$ nanopowder was synthesized using barium carbonate (ACS reagent grade, 99%, Spectrum), strontium carbonate (ACS reagent grade, 99%, Spectrum) and titanium dioxide (ACS reagent grade, 98%, Spectrum) as precursors for barium, strontium and titanium, respectively. The doping insulator materials are Al_2O_3 (ACS reagent grade, Nice, $101.96 \text{ g mol}^{-1}$), ZnO (ACS reagent grade, Merck, 81.37 g mol^{-1}) and MgO (ACS reagent grade, Nice, 40.30 g mol^{-1}). The stoichiometric proportions of $BaCO_3$ and TiO_2 nanopowders were grinded for 1 h. Similarly stoichiometric proportions of $SrCO_3$ and TiO_2 nanopowders were grinded for 1 h. Both mixtures were calcined for 4 h at 1100°C . The melts thus obtained were grinded for 1 h to get $BaTiO_3$ and $SrTiO_3$ nanopowders. Stoichiometric proportions of $BaTiO_3$ and $SrTiO_3$ nanopowders were grinded for 1 h and then calcined for 4 h at 1100°C to get $Ba_{0.7}Sr_{0.3}TiO_3$ nanopowder. Figure 1 shows the procedure for synthesis of 10 g of $Ba_{0.7}Sr_{0.3}TiO_3$.

The synthesized $Ba_{0.7}Sr_{0.3}TiO_3$ sample was blended separately with 0.5, 1.0, 2.0, 4.0 and 8.0 wt% Al_2O_3 . Further, $Ba_{0.7}Sr_{0.3}TiO_3$ sample was blended with 0.5, 1.0, 2.0, 4.0 and 8.0 wt% ZnO and then with 0.5, 1.0, 2.0, 4.0 and 8.0 wt% MgO. After 1 h of blending, all of these samples were calcined for 4 h at 1100°C . The calcined samples were grinded for 1 h in agate mortar. Thus obtained doped $Ba_{0.7}Sr_{0.3}TiO_3$ samples were diepressed into pellets after mixing each sample with the binder (4 wt% aqueous PVA). The pellets were then sintered for 2 h at 1275°C according to sintering cycle shown in Figure 2.

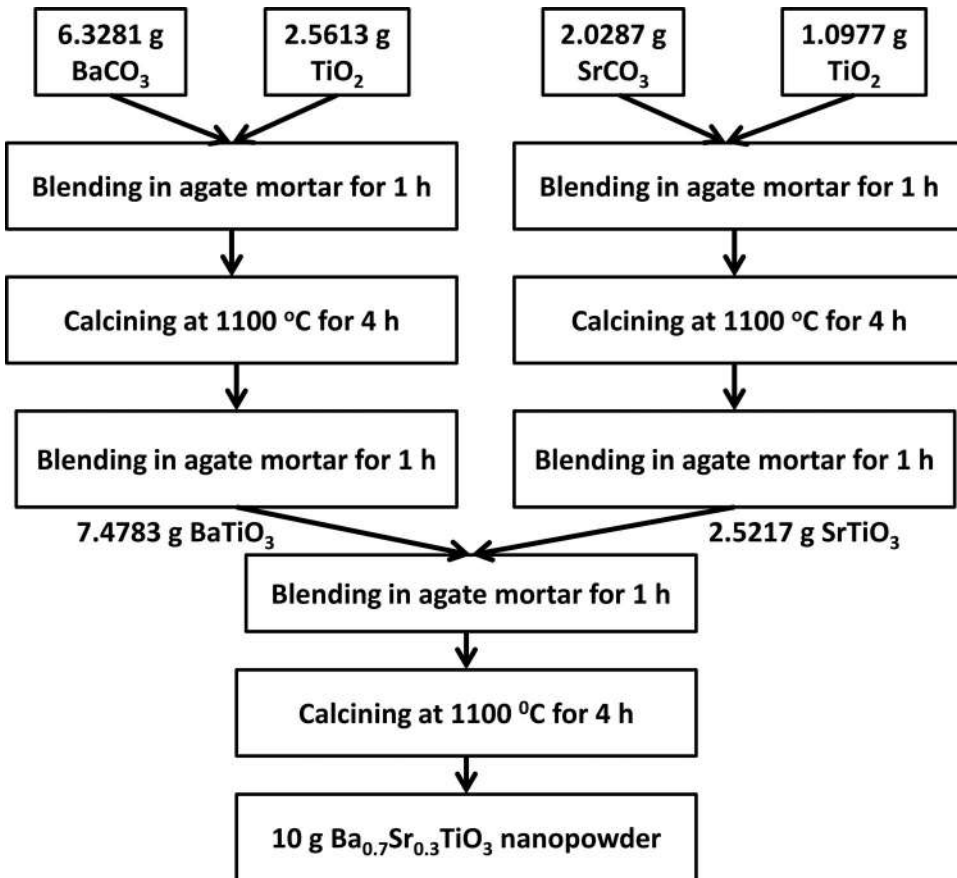


Figure 1. Procedure for synthesis of $\text{Ba}_{0.7}\text{Sr}_{0.3}\text{TiO}_3$.

The mass, diameter and thickness of $\text{Ba}_{0.7}\text{Sr}_{0.3}\text{TiO}_3$ (intrinsic) and $\text{Al}_2\text{O}_3/\text{ZnO}/\text{MgO}$ -doped $\text{Ba}_{0.7}\text{Sr}_{0.3}\text{TiO}_3$ pellets were measured and noted after polishing. Shimadzu AUW220D UniBloc analytical balance was used to measure mass of each pellet. The diameter and thickness of each pellet were measured several times at different positions using Mitutoyo absolute digimatic vernier caliper and mean was taken for further computations.

Further, Ag paste was painted over top and bottom surfaces of pellets to make MIM capacitor. Copper wires at top and bottom electrodes were fixed for capacitor leads. The capacitance of all these pellet MIM capacitors were measured at room temperature using Hioki 3532-50 LCR Hi-Tester. The leakage currents were measured using I-V meter and x-ray powder diffraction patterns were observed using Bruker D8 advance equipment operating with $\text{Cu-K}\alpha$ radiation (40 kV, 40 mA) at step of $2\theta = 0.02^\circ$.

3. Results and Discussion

The performance evaluation of $\text{Al}_2\text{O}_3/\text{ZnO}/\text{MgO}$ -doped $\text{Ba}_{0.7}\text{Sr}_{0.3}\text{TiO}_3$ ceramics based MIM capacitors is discussed in this section. The specific capacitance as well as leakage

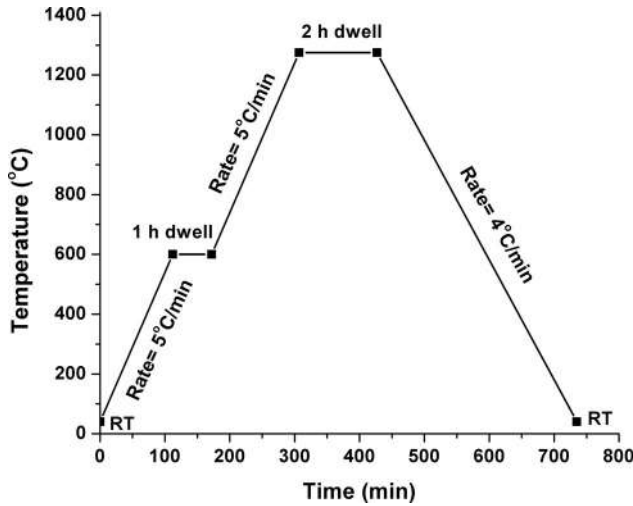


Figure 2. Sintering cycle.

current density of $\text{Al}_2\text{O}_3/\text{ZnO}/\text{MgO}$ -doped $\text{Ba}_{0.7}\text{Sr}_{0.3}\text{TiO}_3$ ceramics based MIM capacitors are evaluated and compared.

3.1. Specific Capacitance

Each green pellet undergoes different area shrinkage during sintering process in accordance with its material contents. Hence specific capacitances are evaluated after fabricating MIM capacitors with these pellets. The specific capacitance of $\text{Al}_2\text{O}_3/\text{ZnO}/\text{MgO}$ -doped $\text{Ba}_{0.7}\text{Sr}_{0.3}\text{TiO}_3$ ceramics based MIM capacitors are evaluated and compared with intrinsic $\text{Ba}_{0.7}\text{Sr}_{0.3}\text{TiO}_3$ ceramics based MIM capacitor.

The concentration of acceptor dopant ions have an effect on growth of crystallite size [4]. There exists a threshold concentration for each dopant ion at which doped $\text{Ba}_{0.7}\text{Sr}_{0.3}\text{TiO}_3$ ceramics based MIM capacitor exhibit highest specific capacitance.

Figure 3 shows the specific capacitances of intrinsic and Al_2O_3 doped $\text{Ba}_{0.7}\text{Sr}_{0.3}\text{TiO}_3$ ceramics based MIM capacitors. The specific capacitance of intrinsic $\text{Ba}_{0.7}\text{Sr}_{0.3}\text{TiO}_3$ ceramic based MIM capacitor is high compared to Al_2O_3 doped $\text{Ba}_{0.7}\text{Sr}_{0.3}\text{TiO}_3$ ceramics based MIM capacitors owing to high relative permittivity of intrinsic $\text{Ba}_{0.7}\text{Sr}_{0.3}\text{TiO}_3$ ceramics compared to that of Al_2O_3 doped $\text{Ba}_{0.7}\text{Sr}_{0.3}\text{TiO}_3$ ceramics. At the same time specific capacitance of intrinsic $\text{Ba}_{0.7}\text{Sr}_{0.3}\text{TiO}_3$ ceramic based MIM capacitor changes with frequency and is not acceptable. 1.0 wt% Al_2O_3 doped $\text{Ba}_{0.7}\text{Sr}_{0.3}\text{TiO}_3$ ceramics based MIM capacitor shows higher specific capacitance than Al_2O_3 doped $\text{Ba}_{0.7}\text{Sr}_{0.3}\text{TiO}_3$ ceramics based MIM capacitors with other doping concentrations of Al_2O_3 which is evident from Figure 3. 1.0 wt% Al_2O_3 doped $\text{Ba}_{0.7}\text{Sr}_{0.3}\text{TiO}_3$ ceramics based MIM capacitor exhibits almost frequency independent specific capacitance as well.

Figure 4 shows the specific capacitances of intrinsic and ZnO doped $\text{Ba}_{0.7}\text{Sr}_{0.3}\text{TiO}_3$ ceramics based MIM capacitors. The specific capacitance of 2.0 wt% ZnO doped $\text{Ba}_{0.7}\text{Sr}_{0.3}\text{TiO}_3$ ceramics based MIM capacitor is higher than that of intrinsic $\text{Ba}_{0.7}\text{Sr}_{0.3}\text{TiO}_3$ ceramic based MIM capacitor and $\text{Ba}_{0.7}\text{Sr}_{0.3}\text{TiO}_3$ ceramics based MIM

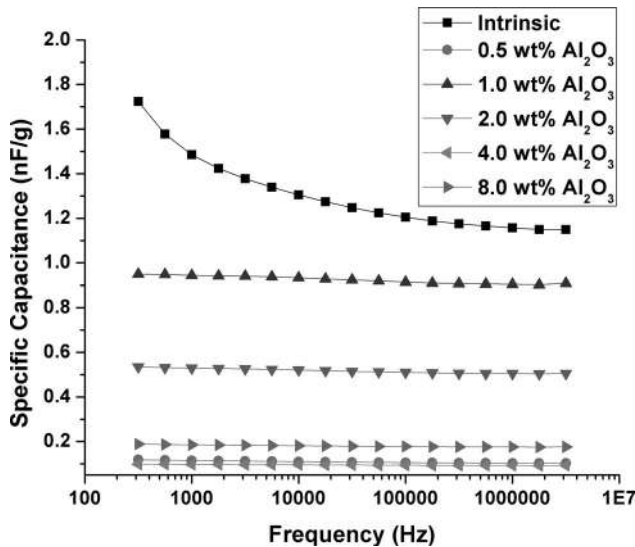


Figure 3. Specific capacitances of intrinsic and Al₂O₃ doped Ba_{0.7}Sr_{0.3}TiO₃ ceramics based MIM capacitors.

capacitors with other doping concentrations of ZnO. Also its specific capacitance is almost stable with frequency.

Figure 5 shows the specific capacitances of intrinsic and MgO doped Ba_{0.7}Sr_{0.3}TiO₃ ceramics based MIM capacitors. The specific capacitance of 4.0 wt% MgO doped Ba_{0.7}Sr_{0.3}TiO₃ ceramics based MIM capacitor is high compared to intrinsic Ba_{0.7}Sr_{0.3}TiO₃ ceramics based MIM capacitor and Ba_{0.7}Sr_{0.3}TiO₃ ceramics based MIM capacitors with other doping concentrations of MgO. Also its specific capacitance is very much stable with frequency compared to intrinsic Ba_{0.7}Sr_{0.3}TiO₃ ceramics based MIM capacitor.

The stability of specific capacitance with frequency can be computed from the slope of specific capacitance versus frequency curves and is given in Table 1. The specific capacitance of 1.0 wt% Al₂O₃ doped Ba_{0.7}Sr_{0.3}TiO₃ ceramics based MIM capacitors is found to be stable with frequency than 2.0 wt% ZnO and 4.0 wt% MgO doped Ba_{0.7}Sr_{0.3}TiO₃ ceramics based MIM capacitors.

Among the intrinsic and Al₂O₃/ZnO/MgO doped Ba_{0.7}Sr_{0.3}TiO₃ ceramics based MIM capacitors investigated in this section, 2.0 wt% ZnO doped Ba_{0.7}Sr_{0.3}TiO₃ ceramics based MIM capacitor exhibits highest specific capacitance of 3 nF g⁻¹ as is evident from Figures 3–5. The stability of specific capacitance with frequency is as good as Al₂O₃ doped Ba_{0.7}Sr_{0.3}TiO₃ ceramics based MIM capacitors.

3.2. Leakage Current Density

The leakage current of intrinsic and Al₂O₃/ZnO/MgO-doped Ba_{0.7}Sr_{0.3}TiO₃ ceramics based MIM capacitors were measured at room temperature. The variation in leakage current density with electric field is studied. Leakage current density versus electric field of intrinsic and Al₂O₃-doped Ba_{0.7}Sr_{0.3}TiO₃ ceramics based MIM capacitors is given in Figure 6. The leakage current performance enhances as Ba_{0.7}Sr_{0.3}TiO₃ ceramics is doped

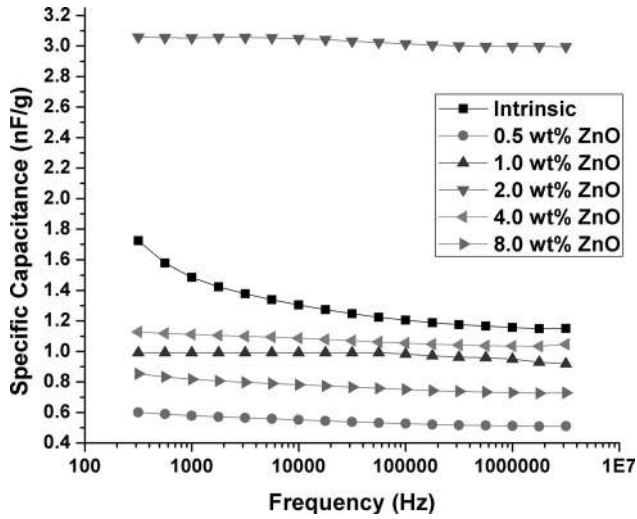


Figure 4. Specific capacitances of intrinsic and ZnO doped $\text{Ba}_{0.7}\text{Sr}_{0.3}\text{TiO}_3$ ceramics based MIM capacitors.

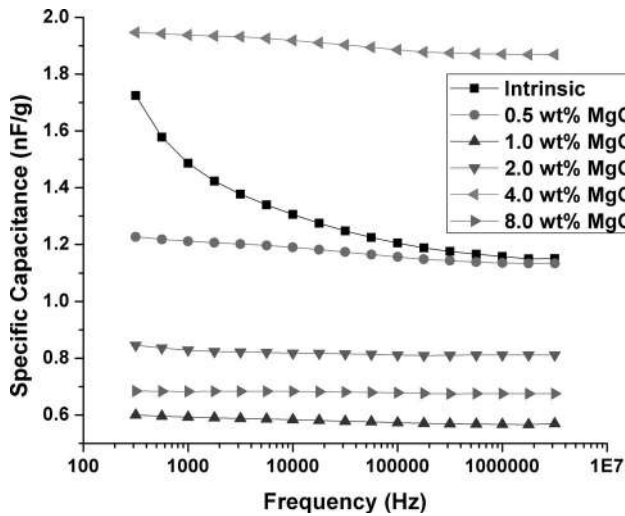


Figure 5. Specific capacitances of intrinsic and MgO doped $\text{Ba}_{0.7}\text{Sr}_{0.3}\text{TiO}_3$ ceramics based MIM capacitors.

with Al_2O_3 which is evident from Figure 6. Also the leakage current density decreases with Al_2O_3 doping concentration. This reduction in leakage current is expected as the band gap of Al_2O_3 is about 8.7 eV which is much higher than that of BST (about 3.9 eV).

Leakage current density versus electric field of intrinsic and ZnO-doped $\text{Ba}_{0.7}\text{Sr}_{0.3}\text{TiO}_3$ ceramics based MIM capacitors is given in Figure 7. When ZnO doping concentration is up to 1.0 wt%, the leakage current is lower than intrinsic $\text{Ba}_{0.7}\text{Sr}_{0.3}\text{TiO}_3$ ceramics based MIM capacitor. As the doping concentration increases, leakage current

Table 1. Computation of variation in specific capacitance with frequency from Figures 3–5.

Doping material	Specific capacitance at 1 kHz (nF)	Specific capacitance at 1 MHz (nF)	Variation in Specific capacitance with frequency (nF decade ⁻¹)
1.0 wt% Al ₂ O ₃	0.944567267	0.904198049	-0.01346
2.0 wt% ZnO	3.053922239	2.997857696	-0.01869
4.0 wt% MgO	1.937650994	1.870005575	-0.02255

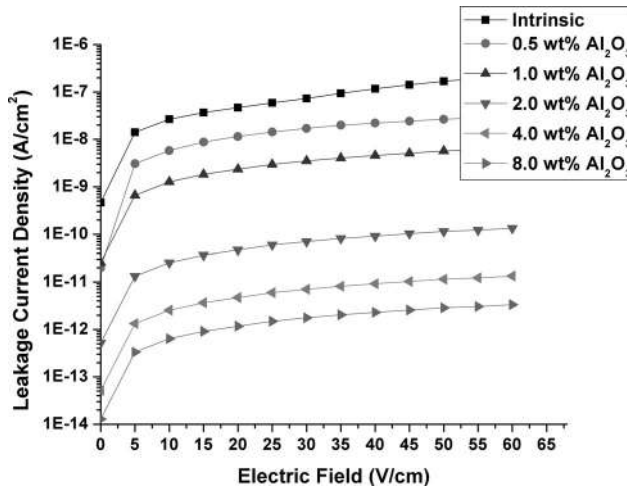


Figure 6. Leakage current density versus electric field of intrinsic and Al₂O₃-doped Ba_{0.7}Sr_{0.3}TiO₃ ceramics based MIM capacitors measured at RT.

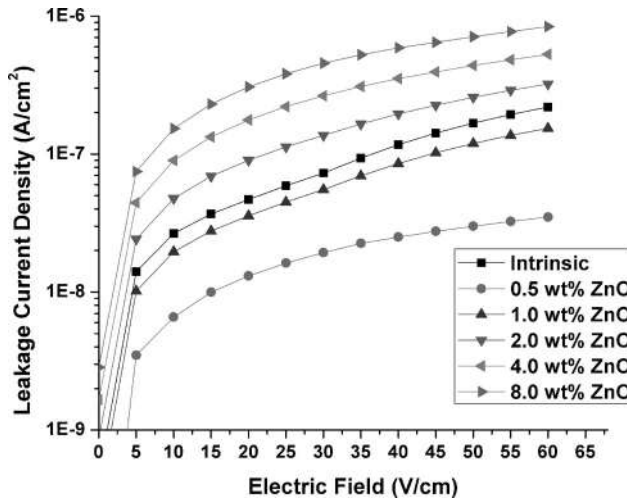


Figure 7. Leakage current density versus electric field of intrinsic and ZnO-doped Ba_{0.7}Sr_{0.3}TiO₃ ceramics capacitors measured at RT.

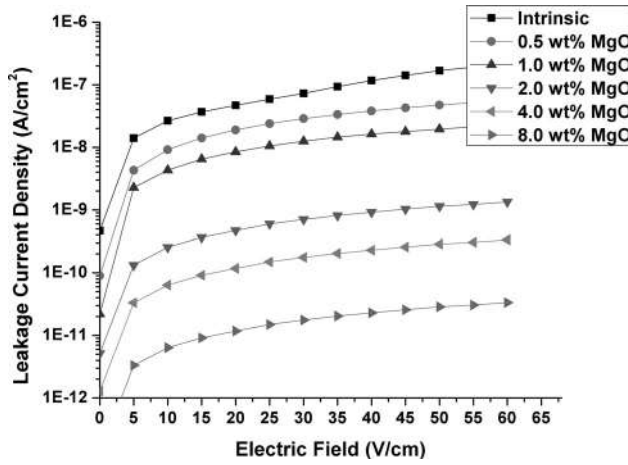


Figure 8. Leakage current density versus electric field of intrinsic and MgO-doped $\text{Ba}_{0.7}\text{Sr}_{0.3}\text{TiO}_3$ ceramics capacitors measured at RT.

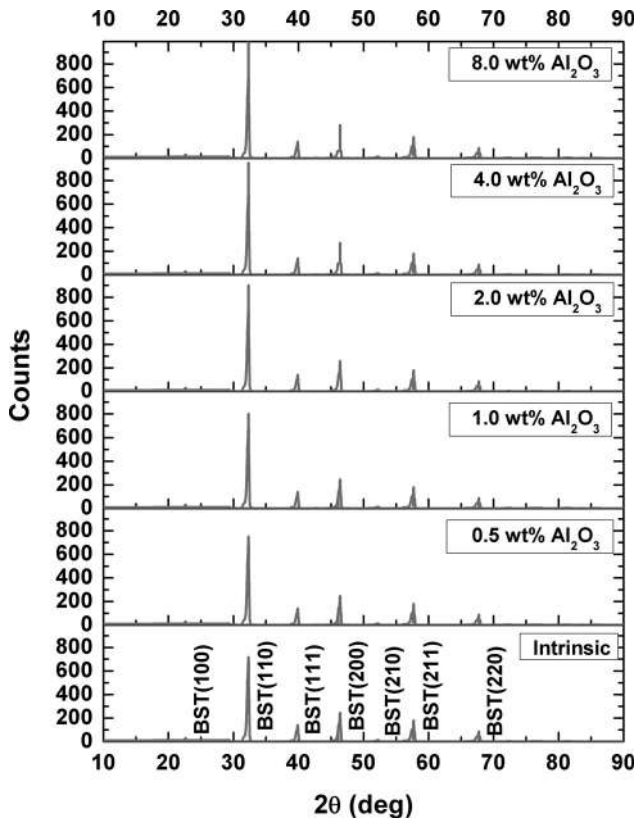


Figure 9. X-ray powder diffraction pattern of intrinsic and Al_2O_3 doped $\text{Ba}_{0.7}\text{Sr}_{0.3}\text{TiO}_3$ ceramics nanopowders.

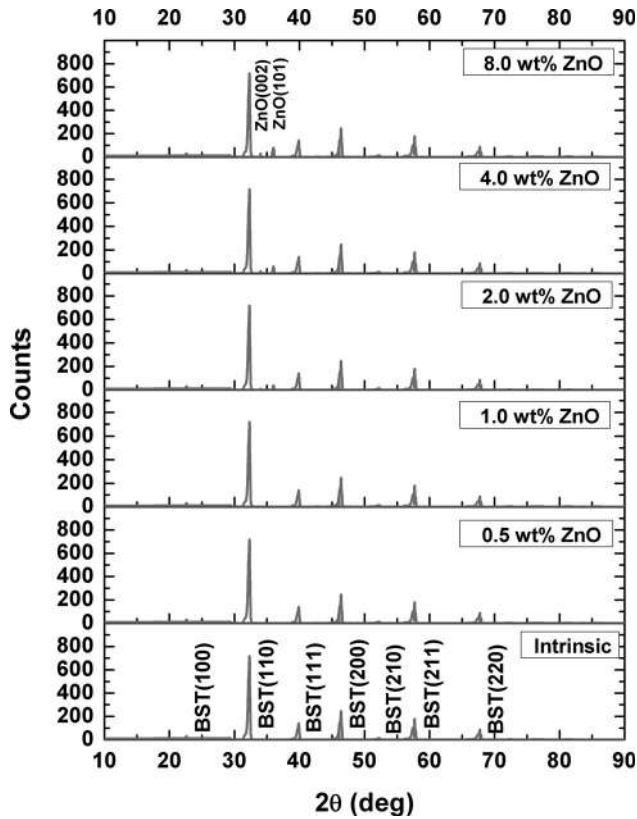


Figure 10. X-ray powder diffraction pattern of intrinsic and ZnO doped $\text{Ba}_{0.7}\text{Sr}_{0.3}\text{TiO}_3$ ceramics nanopowders.

performance deteriorates. This increase in leakage current is expected as the band gap of ZnO is about 3.4 eV which is slightly lower than that of BST.

Leakage current density versus electric field of intrinsic and MgO-doped $\text{Ba}_{0.7}\text{Sr}_{0.3}\text{TiO}_3$ ceramics based MIM capacitors is given in Figure 8. The leakage current performance enhances as $\text{Ba}_{0.7}\text{Sr}_{0.3}\text{TiO}_3$ ceramics is doped with MgO which is evident from Figure 8. Also the leakage current density decreases with MgO doping concentration. This reduction in leakage current is expected as the band gap of MgO is about 5.9 eV which is higher than that of BST.

When the leakage current performance of intrinsic and $\text{Al}_2\text{O}_3/\text{ZnO}/\text{MgO}$ -doped $\text{Ba}_{0.7}\text{Sr}_{0.3}\text{TiO}_3$ ceramics based MIM capacitors for doping concentrations of 0.5 wt%, 1.0 wt%, 2.0 wt%, 4.0 wt% and 8.0 wt% are compared, the leakage current density of 8.0 wt% Al_2O_3 -doped $\text{Ba}_{0.7}\text{Sr}_{0.3}\text{TiO}_3$ ceramics based MIM capacitor is found to be very low which is $3.32 \times 10^{-13} \text{ A cm}^{-2}$ at 5 V cm^{-1} (corresponding to 1.0 V bias). Doping of $\text{Ba}_{0.7}\text{Sr}_{0.3}\text{TiO}_3$ ceramics with MgO is also good for reducing leakage current and the leakage current density of 8.0 wt% MgO-doped $\text{Ba}_{0.7}\text{Sr}_{0.3}\text{TiO}_3$ ceramics based MIM capacitor is $4.12 \times 10^{-12} \text{ A cm}^{-2}$. Further, doping of $\text{Ba}_{0.7}\text{Sr}_{0.3}\text{TiO}_3$ ceramics with ZnO is not sufficient for enhancing leakage current in $\text{Ba}_{0.7}\text{Sr}_{0.3}\text{TiO}_3$ ceramics based MIM capacitors. On considering specific capacitance and leakage current density of 1.0 wt% Al_2O_3 , 2.0 wt% ZnO and 4.0 wt% MgO doped $\text{Ba}_{0.7}\text{Sr}_{0.3}\text{TiO}_3$ ceramics based MIM

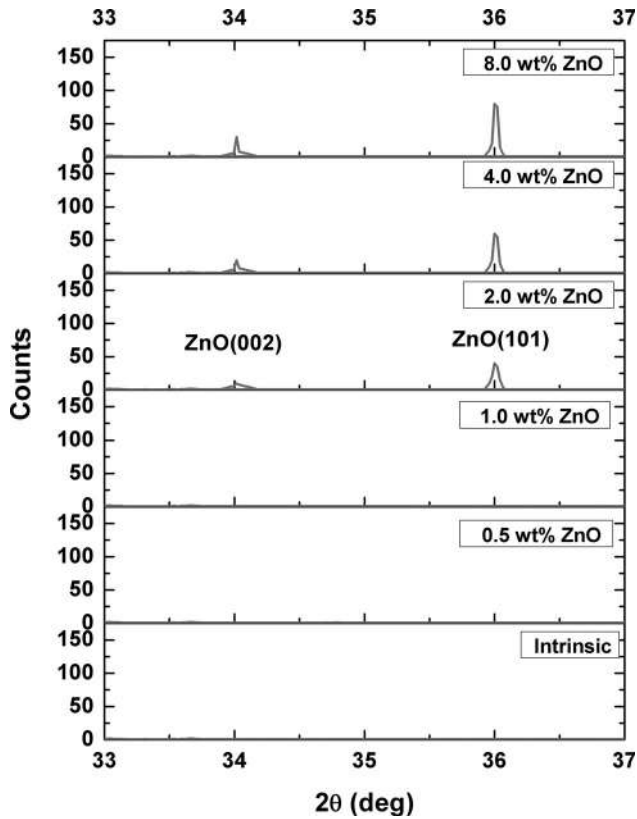


Figure 11. X-ray powder diffraction pattern of intrinsic and ZnO doped Ba_{0.7}Sr_{0.3}TiO₃ ceramics nanopowders for 2θ from 33° to 37°.

capacitors proposed in this work are compared, 4.0 wt% MgO doped Ba_{0.7}Sr_{0.3}TiO₃ ceramics based MIM capacitor is found better for energy storage application.

The leakage current behavior of intrinsic and Al₂O₃/ZnO/MgO-doped Ba_{0.7}Sr_{0.3}TiO₃ ceramics based MIM capacitors are also studied with x-ray powder diffraction pattern which is discussed in section 3.3.

3.3. X-Ray Powder Diffraction

The behavior of leakage current performance of intrinsic and Al₂O₃/ZnO/MgO doped Ba_{0.7}Sr_{0.3}TiO₃ ceramics were studied using x-ray powder diffraction patterns.

XRD patterns of intrinsic and Al₂O₃ doped Ba_{0.7}Sr_{0.3}TiO₃ ceramics nanopowders are shown in Figure 9. The characteristics peaks at diffraction angles $2\theta = 22^\circ, 32^\circ, 40^\circ, 46.5^\circ, 52^\circ, 58^\circ$ and 68° which correspond to BST(100), BST(110), BST(111), BST(200), BST(210), BST(211) and BST(220) respectively [8]. It is also evident from Figure 9 that the prepared samples do not possess any diffraction peaks from doping material (Al₂O₃) phases. This shows that the BST perovskite structure is not altered with Al₂O₃ doping and Al³⁺ ions have entered BST unit cell [4]. As Al₂O₃ doping concentration increases the intensities of diffraction peaks as well as its sharpness increases. This indicates that Ba_{0.7}Sr_{0.3}TiO₃ nanopowder sample attained better crystallinity when Al₂O₃

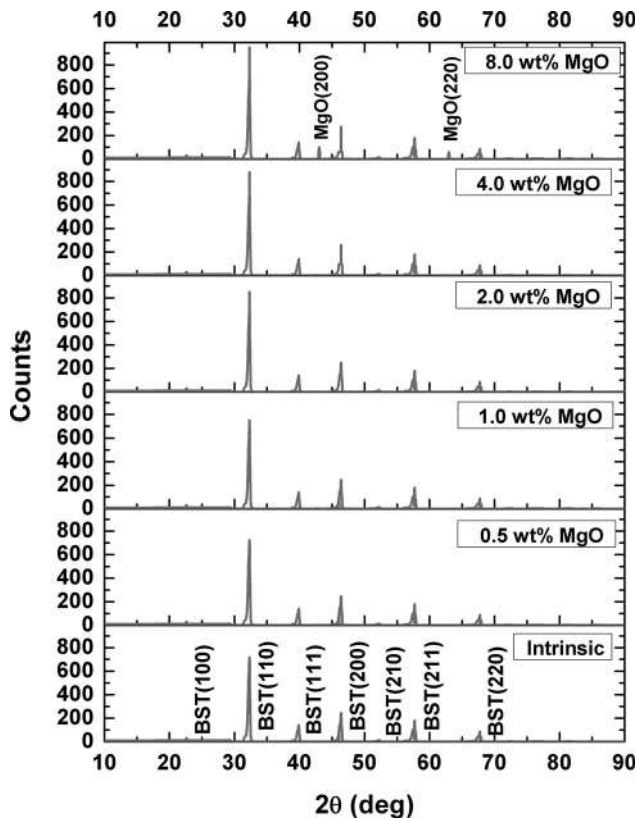


Figure 12. X-ray powder diffraction pattern of intrinsic and MgO doped $\text{Ba}_{0.7}\text{Sr}_{0.3}\text{TiO}_3$ ceramics nanopowders.

doping concentration increases, which justifies the lowering of leakage current (Figure 6).

X-ray powder diffraction patterns of intrinsic and ZnO doped $\text{Ba}_{0.7}\text{Sr}_{0.3}\text{TiO}_3$ ceramics nanopowders are shown in Figure 10. In addition to the characteristics peaks of BST, characteristics peaks of ZnO nanopowder at 34° and 36° corresponds to ZnO(002) and ZnO(101) were also observed.

It is evident from Figure 10 that the ZnO doped $\text{Ba}_{0.7}\text{Sr}_{0.3}\text{TiO}_3$ samples possess characteristics diffraction peaks from ZnO phases from 2.0 wt% doping concentration. X-ray powder diffraction patterns of intrinsic and ZnO doped $\text{Ba}_{0.7}\text{Sr}_{0.3}\text{TiO}_3$ ceramics nanopowders for diffraction angle, 2θ from 33° to 37° are shown in Figure 11. These ZnO characteristics peaks are due to ZnO precipitation as ZnO doping concentration increases. And hence as ZnO doping concentration increases from 2.0 wt%, the leakage current density becomes higher than intrinsic $\text{Ba}_{0.7}\text{Sr}_{0.3}\text{TiO}_3$ sample which is seen in Figure 7.

X-ray powder diffraction patterns of intrinsic and MgO doped $\text{Ba}_{0.7}\text{Sr}_{0.3}\text{TiO}_3$ ceramics nanopowders are shown in Figure 12. In addition to the characteristics peaks of BST, characteristics peaks of MgO nanopowder at 43° and 63° corresponds to MgO(200) and MgO(220) were also observed for 8.0 wt% MgO doped $\text{Ba}_{0.7}\text{Sr}_{0.3}\text{TiO}_3$ ceramics nanopowders.

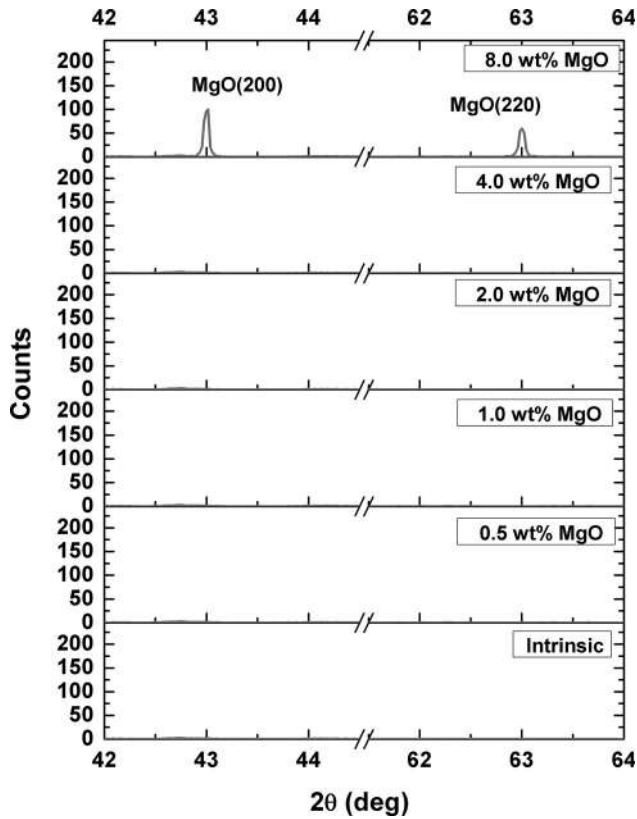


Figure 13. X-ray powder diffraction pattern of intrinsic and MgO doped $\text{Ba}_{0.7}\text{Sr}_{0.3}\text{TiO}_3$ ceramics nanopowders for 2θ from 42° to 44° and 62° to 64° .

X-ray powder diffraction patterns of intrinsic and MgO doped $\text{Ba}_{0.7}\text{Sr}_{0.3}\text{TiO}_3$ ceramics nanopowders for diffraction angle, 2θ from 42° to 44° and 62° to 64° are shown in Figure 13. The characteristic peaks of MgO are observed in MgO doped $\text{Ba}_{0.7}\text{Sr}_{0.3}\text{TiO}_3$ ceramics nanopowders due to MgO precipitation when doping concentration increased to 8.0 wt%. As MgO doping concentration increases the intensities of diffraction peaks of dominant orientations of BST as well as its sharpness increases. This indicates that $\text{Ba}_{0.7}\text{Sr}_{0.3}\text{TiO}_3$ nanopowder sample attained better crystallinity when MgO doping concentration increases, which justifies the lowering of leakage current (Figure 8).

3.4. Performance Comparison

The performance comparison is done with research works in which perovskite insulator materials are doped with metal-oxide dopant materials. In most of the previous research works relative permittivity is given rather than specific capacitance. Hence the performance parameters such as relative permittivity and leakage current density of proposed 4.0 wt% MgO doped $\text{Ba}_{0.7}\text{Sr}_{0.3}\text{TiO}_3$ ceramics based MIM capacitor are compared with related research works and are given in Table 2. The ceramics synthesis methods, insulator materials, dopant materials and its doping concentrations are also given in Table 2.

Table 2. Comparison of performance parameters of proposed capacitor with related research works.

Reference		Synthesis method	Insulator Material	Dopant Material	Doping Concentration	Relative Permittivity	Leakage current density (A cm ⁻²)
Wu et al. (2000)	[9]	Solid state reaction	Ba _{0.6} Sr _{0.4} TiO ₃	Al ₂ O ₃	1 wt%	3200	Not given
Liang et al. (2003)	[4]	Solid state reaction	Ba _{0.6} Sr _{0.4} TiO ₃	Al ₂ O ₃	0.8 wt%	2500	Not given
Hu et al. (2005)	[10]	Solid state reaction	Ba _{0.5} Sr _{0.5} TiO ₃	MgO	20 wt%	450	Not given
Dong et al. (2009)	[11]	Conventional ceramic fabrication	Ba _{0.3} Sr _{0.7} TiO ₃	ZnO	1.6 wt%	610	Not given
Ham et al. (2011)	[12]	Conventional sintering	Ba _{0.5} Sr _{0.5} TiO ₃	LiCO ₃	1 wt%	1441	1.53 × 10 ⁻¹⁰ at 606 V cm ⁻¹
Chou et al. (2012)	[13]	Mixed oxide	Na _{0.5} Bi _{0.5} TiO ₃	ZnO	0.5 wt%	216	Not given
Laishram et al. (2016)	[14]	Conventional ceramic processing	Ba _{0.7} Sr _{0.3} TiO ₃	MgO	10 mol%	2037	Not given
Lu et al. (2017)	[15]	Solid state reaction	0.8BaTiO ₃ -0.2 Bi(Zn _{1/2} Ti _{1/2})O ₃	Nb ₂ O ₅	0.5 wt%	1580	Not given
Hossain et al. (2018)	[16]	Solid oxide	BaTiO ₃	NiO	0.5 wt%	1050	Not given
Panigrahi et al. (2019)	[17]	Mixed oxide reaction	BiFeO ₃ -BaTiO ₃	Ga ₂ O ₃	1.4 mol%	500	Not given
Xu et al. (2020)	[18]	Solid state reaction	0.09AgNbO ₃ -0.01 Bi _{0.5} Na _{0.5} TiO ₃	MnO ₂	0.2 wt%	600	Not given
Proposed work		Solid state reaction	Ba _{0.7} Sr _{0.3} TiO ₃	MgO	4.0 wt%	2035	3.32 × 10 ⁻¹¹ at 5 V cm ⁻¹

Wu et al. [9] achieved a marginal enhancement in relative permittivity compared to the proposed works, but the leakage current performance is not given. Better relative permittivity is obtained for 2.0 wt% ZnO doped Ba_{0.7}Sr_{0.3}TiO₃ ceramics based MIM capacitor compared to the rest of the research works.

In most of the research works, the leakage current density is not provided. Ham et al. [12] achieved a leakage current density better than 1.0 wt% Al₂O₃ and 2.0 wt% ZnO doped Ba_{0.7}Sr_{0.3}TiO₃ ceramics based MIM capacitors. But the relative permittivity as well as leakage current density obtained for 4.0 wt% MgO doped Ba_{0.7}Sr_{0.3}TiO₃ ceramics based MIM capacitor are better than that achieved in [12].

4 Conclusion

The Ba_{0.7}Sr_{0.3}TiO₃ ceramic samples were synthesized using conventional solid-state reaction technique and were doped with 0.5, 1.0, 2.0, 4.0 and 8.0 wt% Al₂O₃, MgO and ZnO. The performance parameters such as specific capacitance and leakage current density of Al₂O₃, ZnO and MgO doped Ba_{0.7}Sr_{0.3}TiO₃ ceramics based MIM capacitors were investigated. The leakage current behavior of all of these capacitors were also studied with x-ray powder diffraction patterns.

It was observed that the specific capacitance of intrinsic Ba_{0.7}Sr_{0.3}TiO₃ ceramic based MIM capacitor changes with frequency. Almost frequency independent specific capacitance was achieved with Al₂O₃ doped Ba_{0.7}Sr_{0.3}TiO₃ ceramics based MIM capacitor. Even though 2.0 wt% ZnO doped Ba_{0.7}Sr_{0.3}TiO₃ ceramics based MIM capacitor exhibits

highest specific capacitance, doping of Ba_{0.7}Sr_{0.3}TiO₃ ceramics with ZnO was not sufficient for enhancing leakage current in Ba_{0.7}Sr_{0.3}TiO₃ ceramics based MIM capacitors. 4.0 wt% MgO doped Ba_{0.7}Sr_{0.3}TiO₃ ceramics based MIM capacitor is found better for energy storage application on investigating specific capacitance and leakage current simultaneously.

Acknowledgments

The authors are grateful to Dr. Surendran K.P. and his research team from Electronic Materials Lab, CSIR-National Institute for Interdisciplinary Science and Technology (NIIST), Thiruvananthapuram, Kerala for their support in carry out experiments.

ORCID

P. S. Smitha  <http://orcid.org/0000-0002-0217-0383>

V. Suresh Babu  <http://orcid.org/0000-0001-8024-2621>

G. Shiny  <http://orcid.org/0000-0002-8907-9389>

References

1. S. B. Herner *et al.*, The effect of various dopants on the dielectric properties of barium strontium titanate, *Mater. Lett* 15 (5-6), 317 (1993).: DOI: [10.1016/0167-577X\(93\)90087-E](https://doi.org/10.1016/0167-577X(93)90087-E).
2. X. Liang, Z. Meng, and W. Wu, Effect of acceptor and donor dopants on the dielectric and tunable properties of barium strontium titanate, *J. American Ceramic Society* 87 (12), 2218 (2004). DOI: [10.1111/j.1151-2916.2004.tb07494.x](https://doi.org/10.1111/j.1151-2916.2004.tb07494.x).
3. M. W. Cole *et al.*, The influence of Mg doping on the materials properties of Ba_{1-x}Sr_xTiO₃ thin films for tunable device applications, *Thin Sol. Fil* 374 (1), 34 (2000).
4. X. Liang, W. Wu, and Z. Meng, Dielectric and tunable characteristics of barium strontium titanate modified with Al₂O₃ addition, *Mater. Sci. Eng.: B* 99 (1-3), 366 (2003). DOI: [10.1016/S0921-5107\(02\)00461-0](https://doi.org/10.1016/S0921-5107(02)00461-0).
5. A. Jain, A. K. Panwar, and A. K. Jha, Effect of ZnO doping on structural, dielectric, ferroelectric and piezoelectric properties of BaZr_{0.1}Ti_{0.9}O₃ ceramics, *Ceram. Int* 43 (2), 1948 (2017).
6. A. S. Attar, E. S. Sichani, and S. Sharafi, Structural and dielectric properties of Bi-doped barium strontium titanate nanopowders synthesized by sol-gel method, *J. Mater. Res. Technol* 6 (2), 108 (2017). DOI: [10.1016/j.jmrt.2016.05.001](https://doi.org/10.1016/j.jmrt.2016.05.001).
7. T. Tsuji, Y. Ohashi, and Y. Yamamura, Effect of ionic radius on electrical conductivity of doped SmAlO₃ perovskite oxide, *Sol. Sta. Ion* 154-155, 541 (2002). DOI: [10.1016/S0167-2738\(02\)00513-1](https://doi.org/10.1016/S0167-2738(02)00513-1).
8. G. Zhu, Z. Yang, and H. Xu, The properties of Ba_{0.5}Sr_{0.5}TiO₃ thin film prepared by RF magnetron sputtering from powder target, *Vacuum* 86 (12), 1883 (2012).
9. L. Wu *et al.*, Direct-current field dependence of dielectric properties in alumina-doped barium strontium titanate, *J. Amer. Ceram. Soc* 83 (7), 1713 (2000). DOI: [10.1111/j.1151-2916.2000.tb01455.x](https://doi.org/10.1111/j.1151-2916.2000.tb01455.x).
10. L. Hu *et al.*, Influence of MgO content on microstructure and dielectric properties in (BaSr)TiO₃ ceramics, *Kem.* 280-283, 85 (2005). DOI: [10.4028/www.scientific.net/KEM.280-283.85](https://doi.org/10.4028/www.scientific.net/KEM.280-283.85).
11. G. Dong *et al.*, Dielectric properties and energy storage density in ZnO-doped Ba_{0.3}Sr_{0.7}TiO₃ ceramics, *Ceram. Int* 35 (5), 2069 (2009).: DOI: [10.1016/j.ceramint.2008.11.003](https://doi.org/10.1016/j.ceramint.2008.11.003).

12. Y.-S. Ham, S. W. Yun, and J.-H. Koh, Analysis on the temperature dependent structural properties of Li_2CO_3 doped $(\text{Ba,Sr})\text{TiO}_3$ ceramics, *J. Electroceram.* 26 (1-4), 32 (2011). DOI: [10.1007/s10832-010-9624-5](https://doi.org/10.1007/s10832-010-9624-5).
13. C.-S. Chou *et al.*, Preparation and characterization of the bismuth sodium titanate ($\text{Na}_{0.5}\text{Bi}_{0.5}\text{TiO}_3$) ceramic doped with ZnO, *Adv. Powder Technol* 23 (3), 358 (2012).
14. R. Laishram, K. C. Singh, and C. Prakash, Enhanced dielectric loss of Mg doped $\text{Ba}_{0.7}\text{Sr}_{0.3}\text{TiO}_3$ ceramics, *Ceram. Int* 42 (13), 14970 (2016). DOI: [10.1016/j.ceramint.2016.06.141](https://doi.org/10.1016/j.ceramint.2016.06.141).
15. Y. Lu *et al.*, Microstructure and dielectric characteristics of Nb_2O_5 doped BaTiO_3 - $\text{Bi}(\text{Zn}_{1/2}\text{Ti}_{1/2})\text{O}_3$ ceramics for capacitor applications, *J. Euro. Ceram. Soc* 37 (1), 123 (2017).
16. T. M. Hossain *et al.*, Fabrication and characterization of NiO-doped BaTiO_3 for multilayer ceramic capacitor, presented at 10th IEEE International Conference on Electrical and Computer Engineering (ICECE), Dhaka, Bangladesh, Bangladesh, Dec 20, 2018, pp. 77–80. DOI: [10.1109/ICECE.2018.8636772](https://doi.org/10.1109/ICECE.2018.8636772).
17. R. Panigrahi *et al.*, Investigation of resistive, capacitive and conductive properties of lead-free electronic material: $0.70\text{Bi}(\text{Fe}_{0.98}\text{Ga}_{0.02})\text{O}_3$ - 0.30BaTiO_3 , *Sol. Sta. Sci* 92, 6 (2019).
18. Y. Xu *et al.*, High energy storage properties of lead-free Mn-doped $(1-x)\text{AgNbO}_3$ - $x\text{Bi}_{0.5}\text{Na}_{0.5}\text{TiO}_3$ antiferroelectric ceramics, *J. Euro. Ceram. Soc* 40 (1), 56 (2020).